Available online at www.sciencedirect.com
SCIENCE DIRECT®
PERGAMON
International Journal of Heat and Mass Transfer 46 (2003) 5073–5085
International Journal of HEAT and MASS TRANSFER
www.elsevier.com/locate/ijhmt

The influence of preferential diffusion and stretch on the burning intensity of a curved flame front with fuel spray

Shuhn-Shyurng Hou [a,*], Jiann-Chang Lin [b]

[a] Department of Mechanical Engineering, Kun Shan University of Technology, Tainan 71003, Taiwan, ROC
[b] Department of General Education, Transworld Institute of Technology, Touliu City, Yunlin County 640, Taiwan, ROC

Received 18 March 2003; received in revised form 18 June 2003

Abstract

In our most recent paper on Bunsen spray flames, only a completely prevaporized mode of a normal Bunsen flame was considered; inverted Bunsen flame and droplet size effects had not been examined yet. In the present study, we consider two flame structures: normal and inverted Bunsen flames, and two spray modes: completely and partially prevaporized burning, by the method of large activation energy asymptotics. In this way, a complete parametric study of flame tip intensification or extinction (opening) can be conducted. Four parameters are used in the analysis. The first two are the droplet size and amount of liquid-fuel loading, which indicate internal heat loss for a rich spray but heat gain for a lean spray. The other two are the stretch and Lewis number (*Le*). Stretch is negative for a normal Bunsen flame but positive for an inverted Bunsen flame. Stretch strengthens (or weakens) the burning intensity of the $Le > 1$ (or $Le < 1$) normal Bunsen flame but decreases (or increases) the burning intensity of the $Le > 1$ (or $Le < 1$) inverted Bunsen flame. Burning intensity of the flame tip intensifies (or weakens) when the lean (or rich) spray has a smaller droplet size or a larger amount of liquid loading. For lean and rich ethanol-spray normal Bunsen flames with $Le > 1$ or a rich methanol-spray inverted Bunsen flame with $Le < 1$, closed-tip solutions are obtained. Conversely, stretch weakens the burning intensities of lean and rich ethanol-spray inverted Bunsen flames with $Le > 1$, or rich methanol-spray normal Bunsen flames with $Le < 1$, eventually leading to tip opening. Moreover, the opening becomes wider (or narrower) as the droplet size decreases or liquid loading increases for the rich (or lean) sprays. Note that for lean ethanol-spray normal (or inverted) Bunsen flame with $Le > 1$, if liquid loading is large enough and droplet size is sufficiently small, there exists flame transition from normal (or inverted) Bunsen through planar to inverted cone (or normal Bunsen) flame. Finally, the critical value of droplet size, at which there exists a planar flame rather than a normal (or an inverted) Bunsen flame, increases with increasing liquid loading.

Keywords: Bunsen flame; Inverted Bunsen flame; Stretch; Lewis number; Tip opening; Spray

1. Introduction

Flame curvature is a significant parameter that influences structure and propagation of premixed flame through its considerable contribution to flame stretch. The Bunsen flame contains a curved premixed reaction zone that has a tip. Using the Bunsen flame as a model curved flame, stretch is manifested through curvature along the surface, attaining its maximum at the tip. There are different stretch rates at different horizontal planes through the Bunsen flame; it also experiences a negative stretch (i.e., compression). Bunsen flame exhibits an interesting phenomenon of local flame extinction, that is, its tip can be either closed or open depending on whether Lewis number (*Le*) is greater than or less than unity [1–6].

Sivashinsky [1,2] was the first to use activation energy asymptotics to analyze the structure of the Bunsen flame tip. Subsequently, Buckmaster [3] explored the

* Corresponding author. Tel.: +886-6-2724833; fax: +886-6-2734240.
E-mail address: sshou@mail.ksut.edu.tw (S.-S. Hou).

0017-9310/$ - see front matter © 2003 Elsevier Ltd. All rights reserved.
doi:10.1016/S0017-9310(03)00362-4

Nomenclature

Dimensional quantities

B'	preexponential factor
C'_{PG}	specific heat of the gaseous mixture
C'_{PL}	specific heat of the liquid
d'	tube diameter
E'_a	activation energy
ℓ'_D	thickness of the diffusion zone
$\overline{\widetilde{M}'}$	average molar mass
$\widetilde{M}'$	molar mass
n'	number density
p'	pressure
$\widetilde{R}$	universal gas constant
r'	droplet radius
S^0_L	one-dimensional adiabatic flame speed

Nondimensional quantities

G	$\mathrm{d}\Phi/\mathrm{d}R$
h_{LG}	latent heat of vaporization, $h'_{LG}/(C'_{PG}T'_i)$
K	$K(T,Y_O)=\ln[1+(T-T_b)/h_{LG}]$ for the vaporizing droplet or $K(T,Y_O)=\ln[1+(T-T_b+Y_OQ)/h_{LG}]$ for the burning droplet
k_F	$k_F=1$ and 0 for the vaporizing droplet and the burning droplet, respectively
k_O	$k_O=0$ and -1 for the vaporizing droplet and the burning droplet, respectively
k_T	$k_T=-h_{LG}$ and $(Q-h_{LG})$ for the vaporizing droplet and the burning droplet, respectively
Le	Lewis number
$\dot{m}$	axial mass flux, ρu
Q	heat combustion of fuel, $Q'/(C'_{PG}T'_i)$
R	radial coordinate, R'/d'
T	temperature, T'/T'_i
T_a	activation temperature, $E'_a/(\widetilde{R}T'_i)$
T_f	adiabatic flame temperature, T'_f/T'_i
u	axial velocity, u'/S^0_L
W	defined in Eq. (7)
x	axial coordinate, x'/d'
Y	$Y_F=Y'_F$ and $Y_O=Y'_O/\sigma$
y	defined in Eq. (1)
z	density variable, ρ'_G/ρ'

Greek symbols

α	$\alpha=1$ and $\alpha=0$ for lean and rich sprays, respectively
β	mass fraction perturbation in the reaction zone
γ	$(1-z_i)/\delta$
δ	small expansion parameter, ℓ'_D/d'
ε	small expansion parameter, T_f/T_a
η	stretched variable of the reaction zone, ξ/ε
θ	temperature perturbation in the reaction zone
Λ	$\Lambda=2(T_f/T_a)(B'\sigma/\widetilde{M}'_O)(p'\overline{\widetilde{M}'}/\widetilde{R})^2\{\lambda'/[C'_{PG}(\rho'_{Gi}S^0_L)^2]\}\exp(-T_a/T_f)$
λ'	thermal conductivity
ξ	stretched variable of the diffusion zone, y/δ
ρ'	density
σ	stoichiometric ratio
τ	$\tau=\{2Le_k\dot{m}_0/[(T_f-1)(Le_k-1)]\}R$
Φ	flame front surface
ϕ	equivalence ratio
ψ	G_0

Superscripts

$'$	dimensional quantities
$+$	downstream near the flame

Subscripts

b	boiling state
c	droplet size for completing vaporization just at the flame front
d	downstream
e	state at which droplet is completely vaporized
F, O	fuel and oxygen
f	flame front
G, L	gas and liquid phases
i	initial state
j	j = F or O
k	k = F and O in lean and rich mixtures, respectively
v	state at which evaporation initiates
w	w = O and F in lean and rich mixtures, respectively
0, 1	zeroth and first orders

mathematical description of open and closed Bunsen flame tips. Both Sivashinsky and Buckmaster concluded that for a negatively stretched Bunsen flame tip, since concave shape with respect to upstream reactants focuses heat ahead of the flame while at the same time defocuses reactants approaching the flame, burning intensity increases for $Le>1$ mixtures but decreases for $Le<1$ mixtures, respectively resulting in the phenomena of tip intensification or extinction (opening). Additionally, some experimental studies [4,5] have reported that observed characteristics of tip opening are in accordance with theoretical predictions [1–3].

The counterpart of the normal Bunsen flame is the inverted Bunsen flame, whose stretch is positive based on curvature alone. The combustion characteristics of inverted Bunsen flames are of great importance and have received much attention [6–10]. For instance, in internal combustion engines, when the initial flames propagate in the swirl flow, the premixed flames are curved and exposed to stretching simultaneously; in some cases, the minute flame structures are the same as the inverted Bunsen flames [7]. Mikolaitis [8,9] studied the interaction of flame curvature and stretch with positive and negative curvatures and found that the flame speed is independent of flame curvature in the absence of stretch. However, the effect of flame curvature is significant in determining changes in flame speed when stretch is present. Recent investigations [6,10] demonstrated that on approaching the flame tip along the surface, burning intensity of the inverted Bunsen flame increases (or decreases) due to the positive curvature coupled with the $Le < 1$ (or $Le > 1$) effect. Therefore, in contrast to normal Bunsen flame, for $Le > 1$ (or $Le < 1$), an inverted Bunsen flame always results in an open-tip (closed-tip) configuration.

The extinction effect of a dispersed phase on premixed flames was first reported by Mitani [11]. Subsequently, much attention has been paid to burning and extinction of dilute spray flames by a series of theoretical studies in one-dimensional models [12–14]. It was concluded that flame extinction characterized by a C-shaped curve is dominated by the external heat loss, while the S-shaped extinction curve is caused by internal heat loss associated with droplet gasification. In those studies, however, the effects of stretch and preferential diffusion on flame behavior were not examined. Recently, Hou and Lin [15,16] formulated an extinction theory of positively stretched premixed flames with a combustible spray in stagnation-point flow. For positively stretched flame, increasing stretch weakens $Le > 1$ flame but intensifies $Le < 1$ flame. It was concluded that external heat loss associated with flow stretch dominates the trend towards flame extinction, and there exists flame flashback rather than flame extinction for rich methanol-spray flame with $Le < 1$.

The studies on normal and inverted Bunsen flames introduced above focused on homogeneous mixtures only. Although coupled influence of positive stretch and combustible spray on planar premixed flames with nonunity Lewis number are available, the literature on negatively stretched Bunsen spray flames or positively stretched inverted Bunsen spray flames is still very limited. Only in our recent study [17], the structure of Bunsen flame tip under the influence of dilute sprays was first reported using large activation energy asymptotics. However, this preliminary study did not include the strong effect of droplet size since it only considered a completely prevaporized mode, in which no liquid droplets existed downstream of the flame. Moreover, the combustion characteristics of inverted Bunsen flames are of great importance but have not been examined yet. Therefore, in the present study, we use large activation energy asymptotics to further analyze the structures of normal and inverted Bunsen flame tips under the influence of droplet size, liquid-fuel loading, preferential diffusion and flame stretch. We consider two flame structures: normal and inverted Bunsen flames, and two spray modes: a completely prevaporized mode and a partially prevaporized mode. In this way, a complete parametric study of flame tip intensification or extinction (opening) can be conducted. We shall also examine the flame front at distances close to the tip of normal (or inverted) Bunsen flames.

2. Theoretical model

2.1. Configuration and assumptions

Fig. 1 shows a schematic diagram of a curved flame front under the influence of a fuel spray. The two-phase premixture consists of gaseous-fuel, air and liquid-fuel droplets. The flow velocity from an infinite distance upstream is uniform along the radial direction and is not refracted by the flame until it crosses the flame. By defining a critical initial droplet size (r'_c) for a droplet to achieve complete evaporation at the premixed flame front, we have completely prevaporized and partially prevaporized spray when $r'_i \leqslant r'_c$ and $r'_i > r'_c$, respectively. Depending on available oxidizer downstream of the flame, the downstream mixture has either droplet burning for lean spray or droplet vaporization for rich

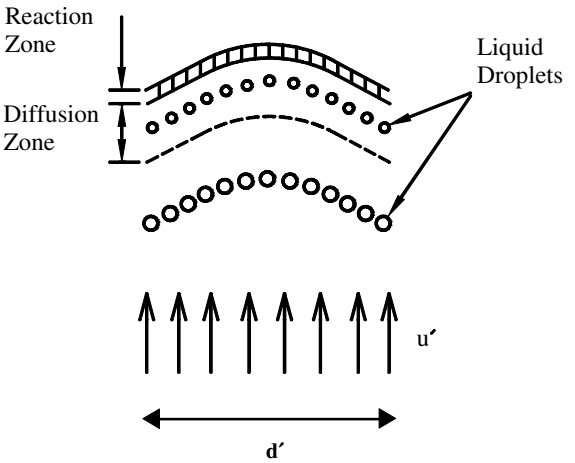

Fig. 1. Schematic diagram of a curved flame front under the influence of a fuel spray.

spray in partially prevaporized mode. Droplets are assumed to start evaporation only when the gas temperature has reached the boiling point of the liquid. In the partially prevaporized mode, droplets then ignite upon crossing the flame, and they vanish upon complete combustion for lean spray or complete evaporation for rich spray.

On the basis of large activation energy asymptotics, we assume that a small parameter $\delta = \ell'_{\rm D}/d' \ll 1$, where $\ell'_{\rm D} = \lambda'/(\rho'_{\rm Gi} C'_{PG} S^0_{\rm L})$ represents the thickness of the diffusion zone and d' denotes the tube diameter; and λ' is thermal conductivity, C'_{PG} is the specific heat at constant pressure, $\rho'_{\rm Gi}$ is the density of the fresh gas at the infinite distance upstream and $S^0_{\rm L}$ is the one-dimensional adiabatic laminar flame speed of a premixed flame. For small tubes, the effect of the boundary layer on the wall of the flame tube could be significant. Our study ignores this effect; therefore it is not valid for small tubes. According to the fast chemical reaction, a thin reaction zone is assumed to be embedded within the diffusion zone. We assume that the spray is monodisperse and dilute, with liquid loading being $O(\varepsilon)$ of total spray mass. Here the small parameter of expansion, ε, is the ratio of thermal energy to large activation energy in the combustion process. Small parameters of δ and ε are assumed to be of the same order for the matching of the reaction zone. Furthermore, at a curved surface a given distance parallel to the flame front, droplets are assumed to be of the same size, droplet temperature is constant and droplet motion is in phase with the gas. Finally, we assume that the fuel and oxidizer reaction for the bulk premixed flame is one-step overall, that droplet gasification follows a d^2-law and that conventional constant property simplifications apply.

2.2. Governing equations

From the assumptions introduced above, the total number of droplets crossing any curved surface parallel to the flame front is constant, i.e., $n'u' = n'_{\rm i}u'_{\rm i}$, where n' is the number density and u' is the axial velocity. We designate the extent of gas-phase heterogeneity by the variable $z = \rho'_{\rm G}/\rho'$, where ρ' is the overall density of the two-phase mixture, such that $z = 1$ represents the completely vaporized state. The characteristic distance and velocity for nondimensionalization are the tube diameter d' and $S^0_{\rm L}$, respectively. Here, quantities with and without primes are dimensional and nondimensional, respectively. After formulating the nondimensional governing equations in the cylindrical coordinate system (R, x) based on cylindrical symmetry, it is convenient to examine the problem by transforming the cylindrical coordinate system (R, x) into the (R, y) coordinate system relative to the surface of the flame front

$$y = x - \Phi(R), \tag{1}$$

where $x = \Phi(R)$ is the equation for the flame front surface. Therefore, the nondimensional equations for overall continuity, gas-phase continuity, and conservation of fuel, oxidizer and energy are, respectively, given by [15–17]:

$$\frac{\partial}{\partial y}(\rho u) = 0, \tag{2}$$

$$\frac{\partial}{\partial y}(z\rho u) = \delta^{-1} A (1-z)^{1/3} (1-z_{\rm i})^{2/3} K(T, Y_{\rm O})/(zT), \tag{3}$$

$$\frac{\partial}{\partial y}(z\rho u Y_{\rm F}) - \delta Le_{\rm F}^{-1}\left\{\frac{\partial^2 Y_{\rm F}}{\partial y^2} + \frac{1}{R}\frac{\partial}{\partial R}\left[R\left(\frac{\partial Y_{\rm F}}{\partial R} - G\frac{\partial Y_{\rm F}}{\partial y}\right)\right] - G\frac{\partial}{\partial y}\left(\frac{\partial Y_{\rm F}}{\partial R} - G\frac{\partial Y_{\rm F}}{\partial y}\right)\right\} = \delta^{-1} W + k_{\rm F}\frac{\partial}{\partial y}(z\rho u), \tag{4}$$

$$\frac{\partial}{\partial y}(z\rho u Y_{\rm O}) - \delta Le_{\rm O}^{-1}\left\{\frac{\partial^2 Y_{\rm O}}{\partial y^2} + \frac{1}{R}\frac{\partial}{\partial R}\left[R\left(\frac{\partial Y_{\rm O}}{\partial R} - G\frac{\partial Y_{\rm O}}{\partial y}\right)\right] - G\frac{\partial}{\partial y}\left(\frac{\partial Y_{\rm O}}{\partial R} - G\frac{\partial Y_{\rm O}}{\partial y}\right)\right\} = \delta^{-1} W + k_{\rm O}\frac{\partial}{\partial y}(z\rho u), \tag{5}$$

$$\frac{\partial}{\partial y}(z\rho u T) - \delta\left\{\frac{\partial^2 T}{\partial y^2} + \frac{1}{R}\frac{\partial}{\partial R}\left[R\left(\frac{\partial T}{\partial R} - G\frac{\partial T}{\partial y}\right)\right] - G\frac{\partial}{\partial y}\left(\frac{\partial T}{\partial R} - G\frac{\partial T}{\partial y}\right)\right\} = -\delta^{-1} WQ + k_{\rm T}\frac{\partial}{\partial y}(z\rho u), \tag{6}$$

where $G = {\rm d}\Phi/{\rm d}R$, $A = 3(\ell'_{\rm D})^2 p' \overline{\widetilde{M}'}/[T'_{\rm i}\rho'_{\rm L}\widetilde{R}(r'_{\rm i})^2]$, and

$$W = -(B'\sigma/\widetilde{M}'_{\rm O})(p'\overline{\widetilde{M}'}/\widetilde{R})^2\{\lambda'/[C'_{PG}(\rho'_{\rm Gi}S^0_{\rm L})^2]\} Y_{\rm O} Y_{\rm F} \times \exp(-T_{\rm a}/T). \tag{7}$$

In Eqs. (3)–(6), the function $K(T, Y_{\rm O})$ and the constant parameters $k_{\rm F}$, $k_{\rm O}$ and $k_{\rm T}$ are, respectively, $\ln[1 + (T - T_{\rm b})/h_{\rm LG}]$, 1, 0 and $-h_{\rm LG}$ for droplet vaporization and $\ln[1 + (T - T_{\rm b} + Y_{\rm O}Q)/h_{\rm LG}]$, 0, −1 and $(Q - h_{\rm LG})$ for droplet burning.

Analysis of the problem will be separated into the following two regions, namely the diffusion zone and the reaction zone. Based on the assumption of ε and δ being of the same order for the matching of the reaction zone, the stretched variables are given by $\xi = y/\delta$ and $\eta = \xi/\varepsilon$ for the diffusion zone and the reaction zone, respectively.

2.3. Diffusion zone

In the diffusion zone, the dependent variables are expanded with respect to the same parameter of δ as

$$T = T_0 + \delta T_1 + O(\delta^2), \tag{8}$$

$$Y_{\rm j} = Y_{\rm j0} + \delta Y_{\rm j1} + O(\delta^2), \quad {\rm j} = {\rm F}, {\rm O}, \tag{9}$$

$$u = u_0 + \delta u_1 + \mathrm{O}(\delta^2), \tag{10}$$

$$\rho = \rho_0 + \delta \rho_1 + \mathrm{O}(\delta^2), \tag{11}$$

$$G = G_0 + \delta G_1 + \mathrm{O}(\delta^2). \tag{12}$$

In order to satisfy the flame structure, z is also expanded as $z = 1 - \delta\gamma z_0 + \mathrm{O}(\delta^2)$ such that $z_\mathrm{i} = 1 - \delta\gamma$ for a dilute spray. Liquid loading is characterized by the parameter γ. Substituting Eqs. (8)–(12) into Eqs. (2), (4)–(6) and expanding, we have

$$\frac{\partial}{\partial\xi}(\rho_0 u_0) = \frac{\partial}{\partial\xi}(\dot{m}_0) = 0, \tag{13}$$

$$\dot{m}_0 \frac{\partial Y_{\mathrm{j}0}}{\partial\xi} - \frac{1}{Le_\mathrm{j}}(1+G_0^2)\frac{\partial^2 Y_{\mathrm{j}0}}{\partial\xi^2} = 0, \quad \mathrm{j} = \mathrm{F},\mathrm{O}, \tag{14}$$

$$\dot{m}_0 \frac{\partial T_0}{\partial\xi} - (1+G_0^2)\frac{\partial^2 T_0}{\partial\xi^2} = 0, \tag{15}$$

from which the zeroth order solutions are readily determined as

$$Y_{\mathrm{j}0} = \begin{cases} Y_{\mathrm{j,i}} - Y_{\mathrm{j,i}} \exp\left(\frac{\dot{m}_0}{1+G_0^2} Le_\mathrm{j}\xi\right), & \mathrm{j} = \mathrm{F},\mathrm{O}, \quad \xi < 0, \\ Y_{\mathrm{j,i}} - Y_{\mathrm{k,i}}, & \xi > 0, \end{cases} \tag{16}$$

$$T_0 = \begin{cases} 1 + (T_\mathrm{f} - 1)\exp\left(\frac{\dot{m}_0}{1+G_0^2}\xi\right), & \xi < 0, \\ T_\mathrm{f}, & \xi > 0, \end{cases} \tag{17}$$

where $\mathrm{k} = \mathrm{F}$ and $\mathrm{k} = \mathrm{O}$ for lean and rich mixtures, respectively. $\dot{m}_0$ denotes axial mass flux.

Using Eqs. (3) and (17), we find

$$z_0 = \left\{ 1 - \frac{2A}{3\dot{m}_0}\int_{\xi_\mathrm{v}}^{\xi} \left[1 + (T_\mathrm{f} - 1)\exp\left(\frac{\dot{m}_0}{1+G_0^2}\xi\right)\right]^{-1} \times \ln\left[1 + \frac{(1-T_\mathrm{b}) + (T_\mathrm{f}-1)\exp\left(\frac{\dot{m}_0}{1+G_0^2}\xi\right)}{h_\mathrm{LG}}\right]\mathrm{d}\xi \right\}^{3/2}, \quad \xi < 0. \tag{18}$$

From Eq. (17), ξ_v represents initiation of droplet evaporation and is given by

$$\xi_\mathrm{v} = [(1+G_0^2)/\dot{m}_0]\ln[(T_\mathrm{b}-1)/(T_\mathrm{f}-1)]. \tag{19}$$

2.4. Reaction zone

In the reaction zone of the bulk gas-phase flame, the solution is expanded around the flame-sheet limit as

$$T = T_\mathrm{f} + \varepsilon T_\mathrm{f}\theta + \mathrm{O}(\varepsilon^2), \tag{20}$$

$$Y_\mathrm{j} = Y_\mathrm{jf} + \varepsilon\beta_\mathrm{j} + \mathrm{O}(\varepsilon^2), \quad \mathrm{j} = \mathrm{F},\mathrm{O}, \tag{21}$$

resulting in

$$Le_\mathrm{j}^{-1}(1+G_0^2)\frac{\partial^2\beta_\mathrm{j}}{\partial\eta^2} = \frac{\Lambda}{2}\left(\frac{T_\mathrm{f}}{T_\mathrm{a}}\right)Y_\mathrm{wd}\beta_\mathrm{k}\exp(\theta), \tag{22}$$

$$-(1+G_0^2)T_\mathrm{f}\frac{\partial^2\theta}{\partial\eta^2} = \frac{\Lambda}{2}Q\left(\frac{T_\mathrm{f}}{T_\mathrm{a}}\right)Y_\mathrm{wd}\beta_\mathrm{k}\exp(\theta), \tag{23}$$

where $\Lambda = 2(T_\mathrm{f}/T_\mathrm{a})(B'\sigma/\widetilde{M}'_\mathrm{O})(p'\overline{\widetilde{M}'}/\widetilde{R})^2\{\lambda'/[C'_{PG}(\rho'_\mathrm{Gi}\times S_\mathrm{L}^0)^2]\}\exp(-T_\mathrm{a}/T_\mathrm{f})$ is the flame speed eigenvalue and $\mathrm{w} = \mathrm{O}$ ($\mathrm{w} = \mathrm{F}$) for lean (rich) mixtures. By using the matching conditions at $\eta \to \pm\infty$, we find

$$T_1(0^+) = -2T_\mathrm{f}\ln\{[(1+G_0^2)^{1/2}/\dot{m}_0][T_\mathrm{f}/(QY_\mathrm{k,i})] \times [\Lambda(T_\mathrm{f}/T_\mathrm{a})Y_\mathrm{wd}Le_\mathrm{k}]^{1/2}\}, \tag{24}$$

in which $T_1(0^+)$ denotes the first-order downstream temperature near the flame. Adding Eq. (4) or (5) to Eq. (6), and then integrating from $\xi = -\infty$ to $\xi = 0^+$ yields

$$T_1(0^+) = \gamma\left\{ T_\mathrm{b} - \frac{C'_{PL}}{C'_{PG}}(T_\mathrm{b}-1) - (T_\mathrm{f} - k_\mathrm{T}) + \frac{\dot{m}_0}{1+G_0^2}(T_\mathrm{f}-k_\mathrm{T})\int_0^{\xi_\mathrm{e}} \exp\left(-\frac{\dot{m}_0}{1+G_0^2}\right)z_0\,\mathrm{d}\xi \right\} - \frac{1}{\dot{m}_0}\frac{(T_\mathrm{f}-1)(Le_\mathrm{k}-1)}{Le_\mathrm{k}}\left(\frac{G_0}{R} + \frac{\mathrm{d}G_0}{\mathrm{d}R}\right), \tag{25}$$

in which

$$\xi_\mathrm{e} = z_0(0)^{2/3}/\{2A\ln[1 + (T_\mathrm{f} - T_\mathrm{b} + \alpha QY_\mathrm{wd})/h_\mathrm{LG})] /(3\dot{m}_0 T_\mathrm{f})\} \tag{26}$$

denotes the completely vaporized state. Here $\alpha = 1$ and $\alpha = 0$ for lean and rich sprays, respectively.

2.5. Final solutions

Combining Eqs. (24) and (25) by eliminating $T_1(0^+)$, and introducing new variables $\psi = G_0$, and $\tau = \{2Le_\mathrm{k}\dot{m}_0/[(T_\mathrm{f}-1)(Le_\mathrm{k}-1)]\}R$, then we have the final results as follows

$$\frac{\mathrm{d}\psi}{\mathrm{d}\tau} + \frac{\psi}{\tau} = T_\mathrm{f}\ln\left\{\frac{(1+\psi^2)^{1/2}}{\dot{m}_0}\frac{T_\mathrm{f}}{QY_\mathrm{k,i}}\left[\Lambda\left(\frac{T_\mathrm{f}}{T_\mathrm{a}}\right)Y_\mathrm{wd}Le_\mathrm{k}\right]^{1/2}\right\} + \frac{\gamma}{2}\left[T_\mathrm{b} - \frac{C'_{PL}}{C'_{PG}}(T_\mathrm{b}-1) - (T_\mathrm{f}-k_\mathrm{T}) + \frac{\dot{m}_0}{1+\psi^2}(T_\mathrm{f}-k_\mathrm{T})\int_0^{\xi_\mathrm{e}} \exp\left(-\frac{\dot{m}_0}{1+\psi^2}\xi\right)z_0\,\mathrm{d}\xi\right]. \tag{27}$$

Here ψ denotes the slope of the surface of the flame front and τ indicates the combined effects of Lewis number and radial position (stretch). The first term on the right hand side of Eq. (27) shows the coupled effects of Lewis number and stretch, while the second term on the right

hand side shows the spray effect, including droplet size (r_i') and liquid-fuel loading (γ).

For the completely prevaporized mode, which was the only mode discussed in the previous investigation [17], the value ξ_e defined in Eq. (26) equals zero, therefore Eq. (27) is simplified as

$$\frac{d\psi}{d\tau}+\frac{\psi}{\tau}=T_f\ln\left\{\frac{(1+\psi^2)^{1/2}}{\dot{m}_0}\frac{T_f}{QY_{k,i}}\left[\Lambda\left(\frac{T_f}{T_a}\right)Y_{wd}Le_k\right]^{1/2}\right\}+\frac{\gamma}{2}\left[T_b-\frac{C'_{PL}}{C'_{PG}}(T_b-1)-(T_f-k_T)\right] \quad (28)$$

indicating that there is no contribution to the flame characteristics coming from the droplet size.

3. Results and discussion

The burning characteristics of two flame structures including normal and inverted Bunsen spray flames are reported and discussed herein. In the analysis, the initial droplet size (r_i') and amount of liquid-fuel loading (γ) indicate the internal heat gain for lean sprays but internal heat loss for rich sprays. Stretch is manifested through curvature along the flame surface of normal (or inverted) Bunsen flame, attaining maximum at the tip. Lewis number designates the ratio of thermal-to-mass diffusivities of the deficient reactant in the mixture. Sample calculations are conducted using Eqs. (24)–(28). A lean ethanol-spray flame ($Le > 1$), a rich ethanol-spray flame ($Le > 1$), and a rich methanol-spray flame ($Le < 1$) are adopted to show the influence of nonunity Lewis number. It is apparent from the parameter $\tau = \{2Le_k\dot{m}_0/[(T_f-1)(Le_k-1)]\}R$ that $\tau > 0$ and $\tau < 0$ correspond to the problems of $Le > 1$ and $Le < 1$, respectively.

It is of interest that by setting $\gamma = 0$, corresponding to the burning of homogeneous mixtures without fuel spray, Eq. (28) degenerates to the result formulated by Sivashinsky [2]. To clearly describe the fuel-spray effect on burning characteristics of normal and inverted Bunsen spray flames in the following sections, it is helpful to show the results of a homogeneous mixture first by using Fig. 2, adopted from the previous report [17]. For $\tau < 0$ ($Le < 1$), a single integral curve (curve A) extends from the negative asymptotic value at $\tau = -\infty$ and decreases monotonically as it approaches the symmetry axis, eventually reaching $\psi = -\infty$ at $\tau = 0$. Therefore, as the tip is approached ($\tau = 0$), the front surface is bent out in such a way that the propagation velocity relative to the oncoming gas falls to zero; that is, a normal Bunsen flame with an open tip for $Le < 1$ is observed. Here ψ denotes the slope of the surface of the flame front. For $\tau > 0$ ($Le > 1$), a cluster of integral curves emanates from the negative asymptotic value at $\tau = +\infty$. Within this family, however, there is only one curve (curve B) corresponding to a closed-tip normal Bunsen flame for which $\psi(0) = 0$. By setting $\gamma = 0$, the integral curves of Eq. (28), for which ψ approaches a positive asymptotic value at $\tau = \pm\infty$, may have an open-tip inverted Bunsen flame (e.g. curve C), when the mixture Lewis number is greater than unity; but a continuous inverted Bunsen flame (e.g. curve D), when the mixture Lewis number is less than unity [2,6].

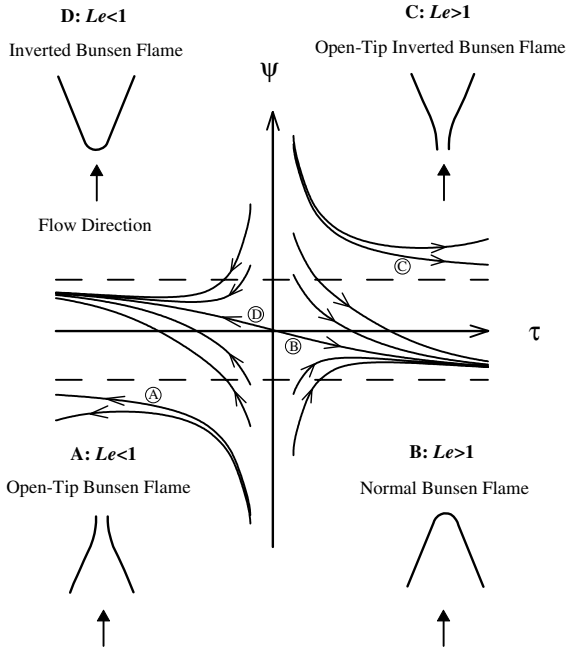

Fig. 2. Phase plane of Eq. (28) with $\gamma = 0$. The arrows on the characteristic curves indicate increasing R (departing from flame tip), i.e., decreasing stretch. Fig. 2 is essentially a reproduction from [2,6].

All of the cases studied herein, listed in Table 1, are discussed in detail in the following.

3.1. Lean ethanol-spray flame with $Le > 1$

The influence of γ and $\dot{m}_0$ on the structure of normal Bunsen flame for lean ethanol–air mixture with completely prevaporized spray are shown in Fig. 3(a). The characteristic curve of $\gamma = 0$ is as expected by Sivashinsky's study [2]. For $Le > 1$ ($\tau > 0$), the curve emanates from the negative asymptotic value at $\tau = +\infty$ and increases monotonically as it approaches the symmetry axis, eventually reaching $\psi = 0$ at $\tau = 0$. Thus, as the tip is approached ($\tau = 0$), the slope (ψ) of the surface of the flame front equals zero, corresponding to a closed-tip normal Bunsen flame. For a fixed γ and a given $\dot{m}_0$, since stretch is manifested through curvature along the normal Bunsen flame surface, ψ increases towards the flame

Table 1
The list of all cases investigated in the study (CPM: completely prevaporized mode; PPM: partially prevaporized mode)

Flame structures	Normal Bunsen flame				Inverted Bunsen flame			
Stretch effects	Negative stretch				Positive stretch			
Mixture types	Lean ethanol spray Rich ethanol spray		Rich methanol spray		Lean ethanol spray Rich ethanol spray		Rich methanol spray	
Lewis number	$Le > 1$		$Le < 1$		$Le > 1$		$Le < 1$	
Flame shapes	Closed tip		Open tip		Open tip		Closed tip	
Spray modes	CPM	PPM	CPM	PPM	CPM	PPM	CPM	PPM
Parameters	γ, $\dot{m}_0$	γ, r_i'	γ, $\dot{m}_0$	γ, r_i'	γ, $\dot{m}_0$	γ, r_i'	γ, $\dot{m}_0$	γ, r_i'

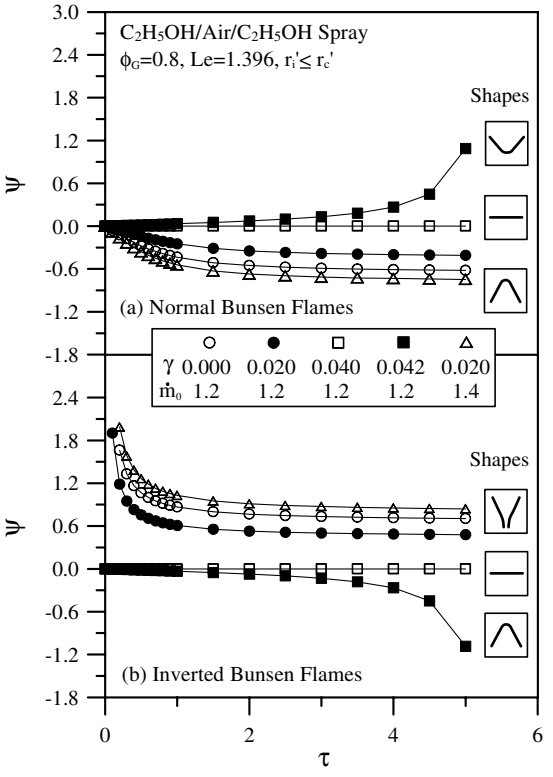

Fig. 3. Influence of liquid loading and axial mass flux on the structure of (a) normal and (b) inverted Bunsen flame for lean ethanol–air mixtures.

tip and attains its maximum at the tip for which $\psi(0) = 0$. The gradual decrease of τ leads to a monotonic increase of ψ and thus results in tip intensification. On the other hand, for a fixed $\gamma = 0.020$, as $\dot{m}_0$ increases from 1.2 to 1.4, the $Le > 1$ flame propagates downstream in order to restore the dynamic equilibrium, thereby decreasing ψ.

As aforementioned, a closed-tip normal Bunsen flame is observed for $Le > 1$ mixture. For droplet gasification in a lean spray, the liquid fuel absorbs heat for upstream prevaporization, produces secondary gasified fuel for bulk gas-phase burning and results in the so-called internal heat gain [12–17], thereby enhancing the burning intensity of the spray flame. At any point in the flame front, local flame velocity equals the component of stream velocity normal to the flame front. At $\dot{m}_0 = 1.2$, with increasing liquid loading (γ), the burning intensity of the lean ethanol–air flame is augmented owing to increased internal heat gain. Therefore, the flame propagates upstream, leading to an increase of ψ at the same radial position. When γ is increased to a critical value ($\gamma^* = 0.040$), the flame moves further upstream and becomes a planar flame (corresponding to $\psi = 0$) rather than a normal Bunsen flame. Furthermore, as $\gamma > \gamma^* = 0.040$, e.g. $\gamma = 0.042$, an inverted cone flame occurs because the value of ψ is positive. Notably, the gradual increase of γ leads to the transition of ψ from negative through zero to positive, corresponding to flame transition from normal Bunsen through planar to inverted cone flame. The parameter γ^* is defined as the critical value of γ at which $\psi = 0$, denoting a planar flame.

For lean ethanol–air mixture with completely prevaporized spray, the influence of γ and $\dot{m}_0$ on the structure of inverted Bunsen flame are shown in Fig. 3(b). Since the tip of inverted Bunsen flame has a convex curvature towards the fresh mixture, it defocuses heat ahead of the flame tip while it simultaneously has a focusing effect on the reactant concentration upstream of the flame tip. Local extinction of inverted Bunsen flame tips is strongly influenced by the coupled effects of stretch and preferential diffusion. For $Le > 1$ ($\tau > 0$), a single integral curve extends from the positive asymptotic value at $\tau = +\infty$ and increases monotonically as it approaches the symmetry axis, eventually reaching $\psi = +\infty$ at $\tau = 0$. Thus, contrary to normal Bunsen flame, as the tip is approached ($\tau = 0$), the front surface is bent out in such a way that the propagation velocity relative to the oncoming gas falls to zero; in other words, an inverted Bunsen flame with an open tip for $Le > 1$ is observed. Additionally, for a fixed $\gamma = 0.020$, as $\dot{m}_0$ increases from 1.2 to 1.4, the $Le > 1$ flame propagates downstream in order to restore dynamic equilibrium, thereby increasing ψ. It is interesting to note that the opening becomes wider with increasing $\dot{m}_0$.

For a given equivalence ratio (ϕ_G) and a given $\dot{m}_0$, the width of the opening decreases with increasing γ because

of additional internal heat gain that results from burning the secondary gasified fuel. When γ is increased to a critical value ($\gamma^* = 0.040$), the flame moves further upstream and becomes a planar flame (corresponding to $\psi = 0$) rather than an open-tip inverted Bunsen flame. Furthermore, as $\gamma > \gamma^* = 0.040$, e.g. $\gamma = 0.042$, the transition from planar flame to closed-tip normal Bunsen flame occurs because the value of ψ is negative, indicating a normal Bunsen flame. Notably, the gradual increase of γ leads to the transition of ψ from positive through zero to negative, corresponding to flame transition from open-tip inverted Bunsen through planar to closed-tip normal Bunsen flame. The parameter γ^* is defined as the critical value of γ at which $\psi = 0$, denoting a planar flame.

Concerning partially prevaporized spray ($r_i' > r_c'$), the influence of initial droplet size on flame characteristics is shown in Fig. 4(a) for lean ethanol-spray normal Bunsen flame of $\phi_G = 0.8$, $\gamma = 0.020$, $Le = 1.396$ and $\dot{m}_0 = 1.2$. It is found that burning intensity decreases with increasing initial droplet size or decreasing stretch (increasing τ). The former is due to reduction of internal heat gain; the latter is caused by augmentation of the $Le > 1$ effect on the negatively stretched flame. A lean spray containing larger droplets with weaker prevaporization upstream of the flame results in reduced internal heat gain and therefore a decreased burning intensity. That is, the weakened flame propagates downstream, leading to a decrease of ψ at the same radial position.

Variation of ψ with τ and r_i' for lean ethanol-spray normal Bunsen flame with $\gamma = 0.042$ at $\dot{m}_0 = 1.2$ is indicated in Fig. 4(b). As shown in Fig. 4(a), at $\gamma = 0.020$ only closed-tip Bunsen flames are obtained. However, at $\gamma = 0.042$, when r_i' is reduced to a critical value ($r_i'^* = 6$ μm), the flame moves further upstream and becomes a planar flame (corresponding to $\psi = 0$) rather than a normal Bunsen flame. Furthermore, when $r_i' < r_i'^* = 6$ μm (partially prevaporized) or $r_i' \leqslant r_c'$ (completely prevaporized), an inverted cone flame occurs because the value of ψ is positive. Note that the gradual decrease of r_i' leads to transition of ψ from negative through zero to positive corresponding to flame transition from normal Bunsen through planar to inverted cone flame. The parameter $r_i'^*$ is defined as the critical value of r_i' at which $\psi = 0$.

The influence of initial droplet size on flame characteristics is shown in Fig. 5(a) and (b) for the lean etha-

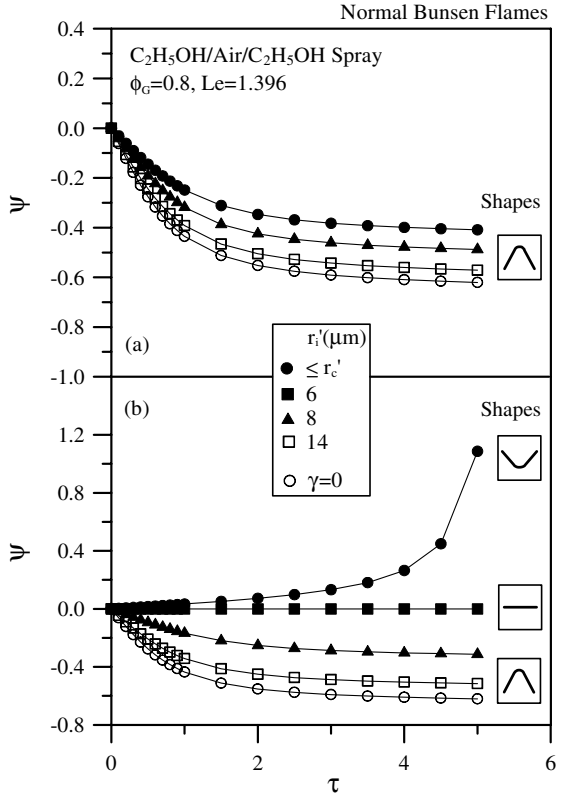

Fig. 4. Influence of initial droplet size on the structure of normal Bunsen flame for lean ethanol–air mixtures with (a) $\gamma = 0.020$ and (b) $\gamma = 0.042$.

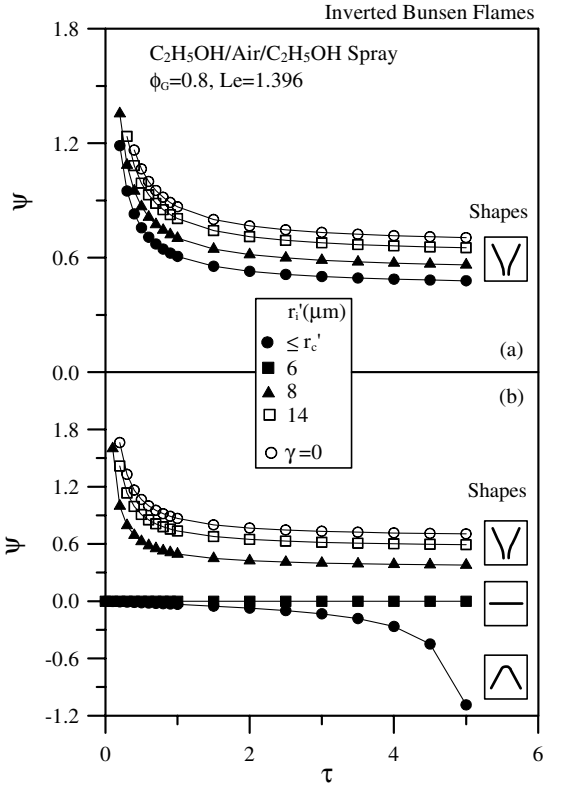

Fig. 5. Influence of initial droplet size on the structure of inverted Bunsen flame for lean ethanol–air mixtures with (a) $\gamma = 0.020$ and (b) $\gamma = 0.042$.

nol-spray inverted Bunsen flame with $\gamma = 0.020$ and $\gamma = 0.042$, respectively. As aforementioned, an inverted Bunsen flame with an open tip is observed for $Le > 1$ mixture. Fig. 5(a) shows that burning intensity decreases with increasing initial droplet size or increasing stretch. The former results from reduction of internal heat gain, the latter results from augmentation of the $Le > 1$ effect on the inverted Bunsen flame which experiences positive stretch. Accordingly, the lean-ethanol spray flame with a larger r_i' propagates downstream, resulting in a ψ increase at the same radial position. Note that only tip opening are found at a smaller liquid loading ($\gamma = 0.020$), as shown in Fig. 5(a), and that the opening becomes wider with increasing r_i'. However, at a larger liquid loading ($\gamma = 0.042$), Fig. 5(b) depicts that the gradual decrease of r_i' results in the transition of ψ from positive through zero to negative, corresponding to flame transition from open-tip inverted Bunsen through planar to closed-tip normal Bunsen flame. The critical value $r_i'^*$, at which $\psi = 0$, is 6 μm as in Fig. 4(b).

The critical value γ^* as a function of $\dot{m}_0$, ϕ_G and $r_i'^*$ for lean ethanol-spray normal Bunsen flames is displayed in Fig. 6. For a fixed equivalence ratio (ϕ_G) with increasing $\dot{m}_0$ (increasing upstream flow velocity), the flame speed required for the occurrence of planar flame is larger. A lean ethanol-spray containing a larger γ has a strengthened burning intensity owing to additional internal heat gain from burning secondary gasified fuel. Therefore, the γ^* value increases with increasing $\dot{m}_0$, as shown in Fig. 6(a). Decrease of ϕ_G, corresponding to reduced burning intensity of the lean ethanol-spray flame, results in the decrease of cone angle (the decrease of ψ). Hence, for a constant $\dot{m}_0 = 1.2$, the γ^* value increases with decreasing ϕ_G, as shown in Fig. 6(b).

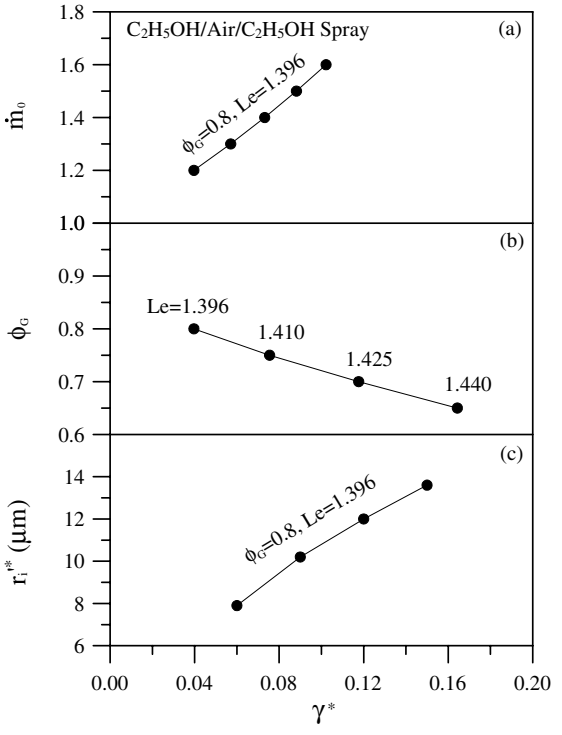

Fig. 6. Critical value γ^* as a function of (a) axial mass flux, (b) equivalence ratio and (c) initial droplet size for normal and inverted lean ethanol–air Bunsen flame.

The critical value $r_i'^*$ as a function of γ^* for a fixed equivalence ratio ($\phi_G = 0.8$) and a constant $\dot{m}_0 = 1.2$ is shown in Fig. 6(c). A lean ethanol-spray flame containing a larger γ or a smaller droplet size has an intensified burning intensity due to additional internal heat gain from burning secondary gasified fuel. With increasing γ^* (increasing burning intensity), the flame propagates further upstream. Therefore, the critical initial droplet ($r_i'^*$) required for the occurrence of planar flame is increased. In other words, a lean ethanol-spray containing larger droplets with weaker prevaporization upstream of the flame results in reduced internal heat gain, and therefore has a weakened burning intensity. Accordingly, the γ^* value required for the occurrence of transition from normal Bunsen flame to planar flame increases with $r_i'^*$.

Note that Fig. 6 is not only valid for normal Bunsen flames but also for inverted Bunsen flames. Contrary to lean ethanol-spray normal Bunsen flame, for lean ethanol-spray inverted Bunsen flame with $Le > 1$, when liquid loading is large enough and initial droplet size is sufficiently small, there exists flame transition from open-tip inverted Bunsen through planar to closed-tip normal Bunsen flame. The critical value of liquid-fuel loading, at which there exists a planar flame rather than an inverted Bunsen flame, increases with increasing initial droplet size, increasing upstream flow velocity, or decreasing equivalence ratio.

3.2. Rich ethanol-spray flame with $Le > 1$

Fig. 7(a) demonstrates the influence of γ and $\dot{m}_0$ on the structure of normal Bunsen flame tip for rich ethanol–air flame ($\phi_G = 1.4$ and $Le = 1.248$) under completely prevaporized conditions. As in the above discussion, a closed-tip normal Bunsen flame is observed for $Le > 1$ mixture. Contrary to the lean spray, the liquid fuel absorbs heat for upstream prevaporization, producing secondary gasified fuel, but there is no oxygen for these fuel vapors to combust in a rich spray according to the assumption that the fuel and oxidizer reaction for the bulk premixed flame is one-step overall. Accordingly, the secondary gasified fuel makes no contribution to burning for the rich spray, resulting in overall internal heat loss [12–17] associated with droplet gasification process, and consequently weakening the burning intensity. Therefore, in order to restore dynamic

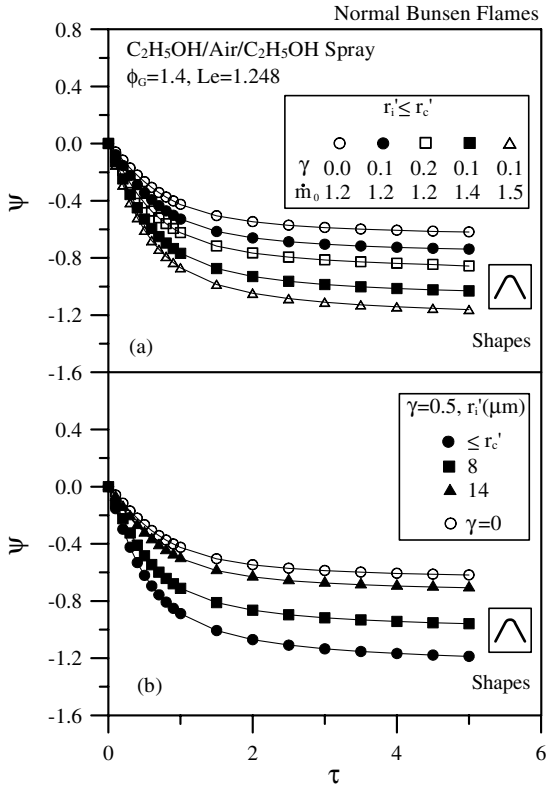

Fig. 7. Influence of (a) liquid loading and axial mass flux, (b) initial droplet size on the structure of normal Bunsen flame for rich ethanol–air mixtures.

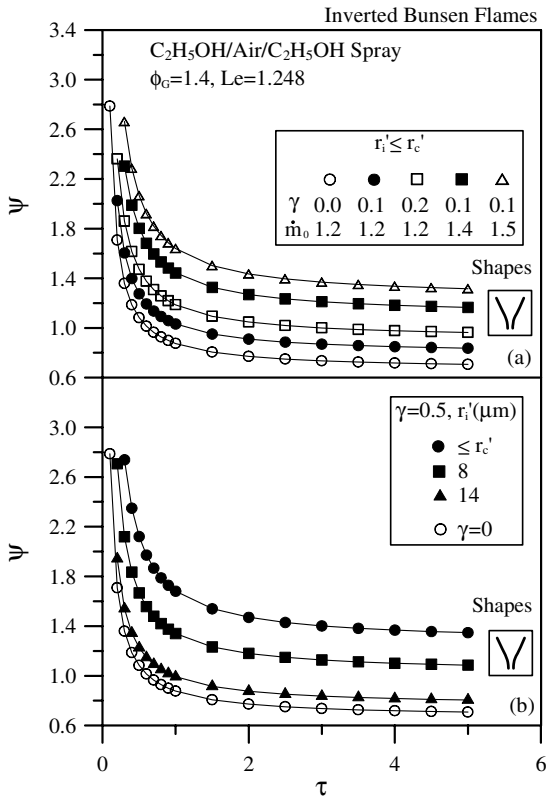

Fig. 8. Influence of (a) liquid loading and axial mass flux, (b) initial droplet size on the structure of inverted Bunsen flame for rich ethanol–air mixtures.

equilibrium, the weakened flame with a larger γ (a larger amount of internal heat loss) moves downstream, resulting in decrease of ψ. At $\gamma = 0.1$, increasing $\dot{m}_0$ (from 1.2 through 1.4 to 1.5) makes the flame move downstream, indicating a decrease of ψ.

Variation of ψ with τ and r_i' for a rich ethanol-spray normal Bunsen flame with a $\gamma = 0.5$ liquid-fuel loading at $\dot{m}_0 = 1.2$ under partially prevaporized conditions is indicated in Fig. 7(b). A rich spray containing larger droplets with weaker prevaporization upstream of the flame results in reduced internal heat loss and therefore an intensified burning intensity. Hence, the flame propagates upstream, leading to an increase of ψ at the same radial position. Notably, burning intensity of rich ethanol-spray flame is intensified with decreasing γ (Fig. 7a) or increasing r_i' (Fig. 7b). On the other hand, ψ increases with increasing stretch (decreasing τ), caused by the augmentation of the $Le > 1$ effect on the negatively stretched flame.

Fig. 8(a) shows the influence of γ and $\dot{m}_0$ on the structure of inverted Bunsen flame tip for rich ethanol–air flame ($\phi_G = 1.4$ and $Le = 1.248$) under completely prevaporized conditions. It is well known that open-tip solutions should be obtained for $Le > 1$ inverted Bunsen flame. For a given $\dot{m}_o$, the burning intensity decreases (ψ increases) with increasing γ or decreasing τ (increasing stretch). For fixed γ, an increase of $\dot{m}_0$ leads to increasing ψ since the flame shifts further downstream to restore dynamic equilibrium. Fig. 8(b) displays the influence of r_i' on the structure of inverted Bunsen flame tip for rich ethanol-spray flame at $\dot{m}_0 = 1.2$ under partially prevaporized conditions. A rich spray containing smaller droplets with stronger prevaporization upstream of the flame results in increased internal heat loss and therefore a decreased burning intensity (an increased ψ). It is seen that tip opening becomes wider when the liquid loading (γ) or upstream flow velocity ($\dot{m}_0$) increases (Fig. 8a), or initial droplet size (r_i') decreases (Fig. 8b).

3.3. Rich methanol-spray flame with $Le < 1$

Only the rich methanol-spray flame is discussed here because both lean methanol- and ethanol-spray flames ($Le > 1$) have similar flame behavior. Fig. 9(a) shows the influence of γ and $\dot{m}_0$ on the structure of normal Bunsen flame for rich methanol–air mixtures ($\phi_G = 1.4$ and

$Le = 0.971$) under completely prevaporized conditions. For $Le < 1$ ($\tau < 0$), a single integral curve for $\gamma = 0$ extends from the negative asymptotic value at $\tau = -\infty$ and decreases monotonically as it approaches the symmetry axis, eventually reaching $\psi = -\infty$ at $\tau = 0$. Thus, as the tip is approached ($\tau = 0$), the front surface is bent out in such a way that the propagation velocity relative to the oncoming gas falls to zero. In other words, contrary to the rich ethanol-spray normal Bunsen flame ($Le > 1$) with a closed tip, a rich methanol-spray normal Bunsen flame ($Le < 1$) with an open tip is observed. However, similar to the rich ethanol-spray, the secondary gasified fuel makes no contribution to burning for a rich methanol-spray, thus resulting in overall internal heat loss and subsequently weakening burning intensity of the flame. Therefore, the rich methanol-spray flame ($Le < 1$) has a decreased burning intensity (or a diminished ψ) when the liquid loading (γ) increases. Moreover, ψ decreases with increasing stretch (increasing τ), caused by augmentation of the $Le < 1$ effect on the negatively stretched flame.

Variation of ψ with τ and r_i' at $\gamma = 0.5$ and $\dot{m}_0 = 1.2$ for rich methanol-spray normal Bunsen flame under partially prevaporized conditions is indicated in Fig. 9(b). It is found that with increasing r_i', the characteristic curve for partially prevaporized spray deviates from completely prevaporized spray ($r_i' \leqslant r_c'$) and approaches that for a homogeneous mixture ($\gamma = 0$). This phenomenon illustrates that ψ increases with increasing initial droplet size due to reduction of internal heat loss. In addition, burning intensity decreases when rich spray contains smaller initial droplet size, so that the normal Bunsen flame has a wider open tip. Notably, for rich methanol-spray normal Bunsen flame with $Le < 1$, tip opening becomes wider when γ or $\dot{m}_0$ increases (Fig. 9a), or r_i' decreases (Fig. 9b).

Fig. 10(a) shows the influence of γ and $\dot{m}_0$ on the structure of inverted Bunsen flame tip for rich methanol–air flame ($\phi_G = 1.4$ and $Le = 0.971$) under completely prevaporized conditions. It is seen that closed-tip solutions are obtained for $Le < 1$ inverted Bunsen flame. For a given $\dot{m}_0$, burning intensity decreases (ψ increases) with increasing γ or decreasing τ (decreasing stretch). For a fixed γ, increase of $\dot{m}_0$ leads to increasing ψ since the flame shifts further downstream to restore dynamic equilibrium. Fig. 10(b) illustrates the influence of r_i' on the

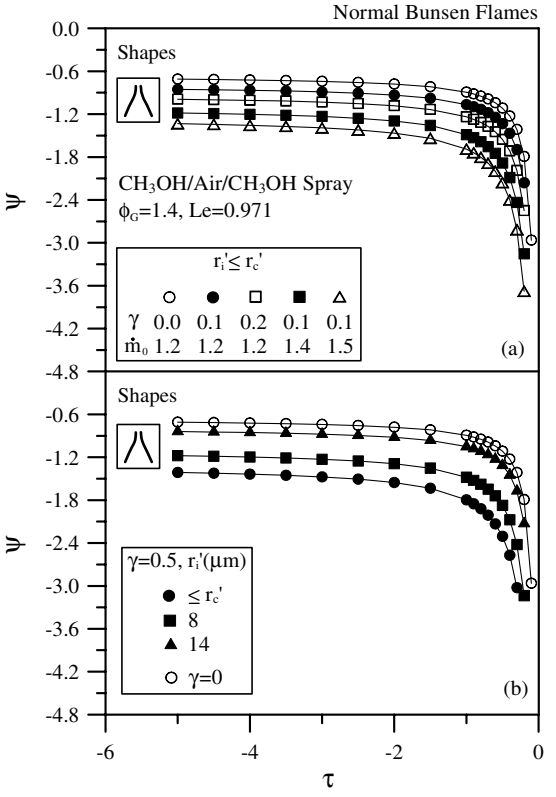

Fig. 9. Influence of (a) liquid loading and axial mass flux, (b) initial droplet size on the structure of normal Bunsen flame for rich methanol–air mixtures.

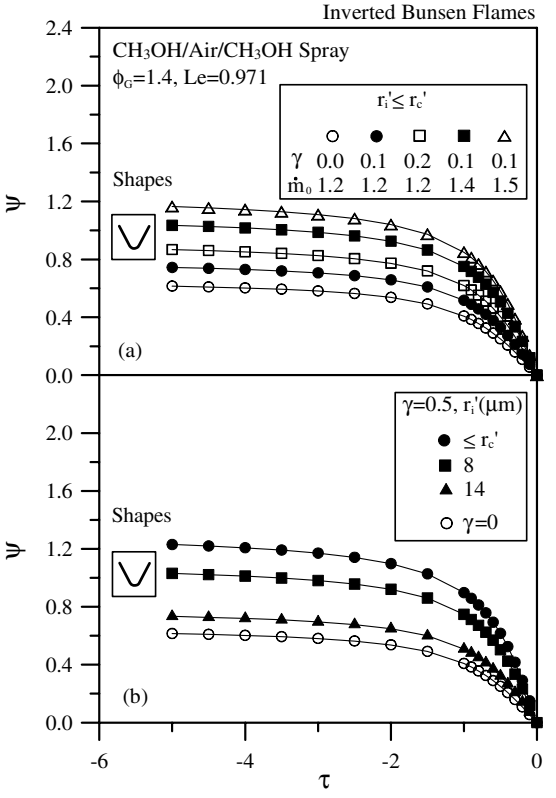

Fig. 10. Influence of (a) liquid loading and axial mass flux, (b) initial droplet size on the structure of inverted Bunsen flame for rich methanol–air mixtures.

structure of inverted Bunsen flame tip for rich methanol-spray flame ($\phi_G = 1.4$, $Le = 0.971$ and $\dot{m}_0 = 1.2$). A rich spray containing larger droplets with weaker prevaporization upstream of the flame results in reduced internal heat loss, and therefore an intensified burning intensity. Hence, the strengthened flame propagates further upstream, corresponding to ψ decrease. Note that burning intensity becomes stronger when γ decreases (Fig. 10a), or r_i' increases (Fig. 10b) for rich spray flame.

4. Conclusions

A theory of stretched premixed flame with combustible spray was further developed using activation energy asymptotics to explore the influence of droplet size, liquid-fuel loading, flame stretch and Lewis number on the structure of normal and inverted Bunsen flame tips. The results are summarized as follows:

1. For lean and rich ethanol-spray flames with $Le > 1$, closed-tip solutions for a normal Bunsen flame and open-tip solutions for an inverted Bunsen flame can be obtained. Conversely, for rich methanol-spray flames ($Le < 1$), there are two possible configurations, a normal Bunsen flame with an open tip and a continuous inverted Bunsen flame with a closed tip.

2. Internal heat transfer embedded in lean (or rich) spray results in overall internal heat gain (or heat loss) for the system. Therefore, the burning intensity of lean (or rich) spray flame increases (or decreases) with decreasing initial droplet size or increasing liquid loading.

3. Considering the lean ethanol-spray normal Bunsen flame with $Le > 1$, burning intensity enhancement by the negative stretch can be further increased when the spray contains increased liquid-fuel loading or decreased initial droplet size. However, if liquid-fuel loading is large enough, the gradual decrease in initial droplet size leads to flame transition from closed-tip normal Bunsen through planar to closed-tip inverted cone flame. The critical value of liquid-fuel loading, at which there exists a planar flame rather than a normal Bunsen flame, increases with increasing initial droplet size or upstream flow velocity, or decreasing equivalence ratio.

4. Contrary to lean ethanol-spray normal Bunsen flame, for lean ethanol-spray inverted Bunsen flame with $Le > 1$, when liquid loading is large enough and initial droplet size is sufficiently small, there exists flame transition from open-tip inverted Bunsen through planar to closed-tip normal Bunsen flame. Moreover, the critical value of liquid-fuel loading, at which there exists a planar flame rather than an inverted Bunsen flame, increases with increasing initial droplet size or upstream flow velocity, or decreasing equivalence ratio.

5. Stretch weakens burning intensity of lean (or rich) ethanol-spray inverted Bunsen flame with $Le > 1$ and eventually leads to tip opening, i.e., flame extinction. The burning intensity of lean (or rich) ethanol-spray inverted Bunsen flame decreases (or increases) with increasing initial droplet size or decreasing liquid loading. Note that the tip opening of lean (or rich) ethanol-spray inverted Bunsen flame becomes wider (or narrower) with increasing initial droplet size, increasing (or decreasing) upstream flow velocity, or decreasing liquid loading.

6. The burning intensity of rich methanol-spray inverted Bunsen flame with a closed tip decreases when droplet size decreases or liquid-fuel loading increases. Moreover, the opening of rich methanol-spray normal Bunsen flame tip widens with decreasing initial droplet size, or increasing liquid-fuel loading or upstream flow velocity. Note that flame transition from normal (or inverted) Bunsen through planar to inverted cone (or normal Bunsen) flame does not occur for the rich methanol-spray flame with $Le < 1$.

Acknowledgements

The authors would like to thank the National Science Council, Taiwan, ROC, for financially supporting this research under Contract of NSC 91-2212-E-168-014. Valuable comments by the reviewers of this report are kindly appreciated.

References

[1] G.I. Sivashinsky, The diffusion stratification effect in Bunsen flames, J. Heat Transfer 96 (1974) 530–535.
[2] G.I. Sivashinsky, Structure of Bunsen flames, J. Chem. Phys. 62 (2) (1975) 638–643.
[3] J. Buckmaster, A mathematical description of open and closed flame tip, Combust. Sci. Technol. 20 (1979) 33–40.
[4] C.K. Law, S. Ishizuka, P. Cho, On the opening of premixed Bunsen flame tips, Combust. Sci. Technol. 28 (1982) 89–96.
[5] M. Mizomoto, Y. Asaka, S. Ikai, C.K. Law, Effects of preferential diffusion on the burning intensity of curved flames, in: Proceedings of the Twentieth Symposium (International) on Combustion, The Combustion Institute, 1984, pp. 1933–1939.
[6] C.J. Sung, K.M. Yu, C.K. Law, On the geometry and burning intensity of Bunsen flames, Combust. Sci. Technol. 100 (1994) 245–270.
[7] K. Asato, T. Kawamura, T. Ban, Effects of curvature on extinction of premixed flames stabilized in stagnation flow, in: Proceedings of the Twenty-Second Symposium (International) on Combustion, The Combustion Institute, 1988, pp. 1509–1515.
[8] D.W. Mikolaitis, The interaction of flame curvature and stretch. Part 1: The concave premixed flame, Combust. Flame 57 (1984) 25–31.

[9] D.W. Mikolaitis, The interaction of flame curvature and stretch. Part 2: The convex premixed flame, Combust. Flame 58 (1984) 23–28.
[10] C.K. Law, C.J. Sung, Structure, aerodynamics, and geometry of premixed flamelets, Prog. Energy Combust. Sci. 26 (2000) 459–505.
[11] T. Mitani, A flame inhibition theory by inert dust and spray, Combust. Flame 43 (1981) 243–253.
[12] C.C. Liu, T.H. Lin, The interaction between external and internal heat losses on the flame extinction of dilute sprays, Combust. Flame 85 (1991) 468–478.
[13] S.S. Hou, C.C. Liu, T.H. Lin, The influence of external heat transfer on flame extinction of dilute sprays, Int. J. Heat Mass Transfer 36 (1993) 1867–1874.
[14] S.S. Hou, T.H. Lin, A theory on excess-enthalpy spray flame, Atomization Spray. 9 (1999) 355–369.
[15] S.S. Hou, T.H. Lin, Extinction of stretched spray flames with nonunity Lewis numbers in a stagnation-point flow, in: Proceedings of the Twenty-Seventh Symposium (International) on Combustion, The Combustion Institute, 1998, pp. 2009–2015.
[16] S.S. Hou, T.H. Lin, Effects of internal heat transfer and preferential diffusion on stretched spray flames, Int. J. Heat Mass Transfer 44 (2001) 4391–4400.
[17] J.C. Lin, S.S. Hou, T.H. Lin, A theoretical study on Bunsen spray flames, Int. J. Heat Mass Transfer 46 (2003) 963–971.